Control of Gilbert damping using magnetic metamaterials

Chiharu Mitsumata*
Department of Electronic Engineering, Graduate School of Engineering, Tohoku University, Aoba, Sendai 980-8579, Japan

Satoshi Tomita†
Graduate School of Materials Science, Nara Institute of Science and Technology (NAIST), Ikoma, Nara 630-0192, Japan
(Received 8 April 2011; revised manuscript received 7 October 2011; published 18 November 2011)

We studied, from a theoretical standpoint, the Landau-Lifshitz-Gilbert equation of magnetic metamaterials consisting of magnetic nanoparticles. The dynamics of the metamaterials magnetization was numerically investigated in order to elucidate the mechanism of Gilbert damping. Our results revealed that the interacting dipole field synchronized to the magnetization precession causes the variation in the effective Gilbert damping factor. Nevertheless, we found that a metamaterial with a specific structure has almost the identical effective Gilbert damping factor, although the interacting dipole field increases. This work demonstrates that the effective Gilbert damping factor can be analytically predicted and designed using the structure factors in magnetic metamaterials, opening an avenue to a new relationship between metamaterials and spintronics.

DOI: 10.1103/PhysRevB.84.174421 PACS number(s): 78.67.Pt, 75.75.Jn, 76.50.+g

I. INTRODUCTION

Artificial structures consisting of subunits much smaller than the wavelength of electromagnetic waves are called metamaterials.[1] As well as split-ring resonators using nonmagnetic metals,[2,3] magnetic metamaterials consisting of magnetic metal, for example, nickel, cobalt, or iron, nanoparticles are one of the candidates for obtaining magnetic resonance and tailoring magnetic permeability (μ) in the microwave region.[4] The μ represents how strong the material respond to dynamic magnetic field. Therefore, a clear understanding of the magnetization dynamics of magnetic metamaterials under a dynamic magnetic field is crucial for tailoring μ.

Damping is a key issue to understanding the dynamics of magnetization. The magnetization damping can be represented using the so-called Gilbert damping factor α, which is phenomenologically introduced in the motion equation of magnetization or spin, i.e., the Landau-Lifshitz-Gilbert (LLG) equation.[5] However, the physical origin of magnetization damping represented by α has only recently been addressed. This address is mainly motivated by spin damping in spintronics,[6–10] which utilize the spins of electrons for information delivery and storage, because spin damping is strongly related to the spin reversal time. Because μ strongly depends on α, the control of α is important also for magnetic metamaterials.

Previously we reported the preparation of magnetic metamaterials consisting of nickel nanoparticles and magnetic resonance around 10 GHz due to the electron spins [electron magnetic resonance (EMR)] in the particles.[11–13] Measured EMR signals were theoretically considered and μ of the metamaterials was numerically evaluated by precisely taking the dipole field among nanoparticles into consideration.[14,15] These studies pointed out a limitation of the static approximation based on Kittel's equation[16] and the importance of the dynamic approximation for evaluating μ of magnetic metamaterials. Nevertheless, the physics of the dynamic approximation and Gilbert damping in the metamaterials was unclear.

In this paper, we report theoretical considerations of the LLG equation in the magnetic metamaterials and numerical calculation of the magnetization dynamics in order to shed light on the physics of the dynamic approximation and Gilbert damping in the magnetic metamaterials. Our results reveal that an interacting dipole field, which is synchronized to the precession of magnetization, causes the variation in the effective Gilbert damping factor. Nevertheless, it is noticeable that a metamaterial consisting of dual-sized particles has almost the same effective Gilbert damping factor with that of single-sized particles, even though there is an increase in the interacting dipole field. These results indicate that the interacting dipole field intricately influences the effective Gilbert damping factor through the structure factors. Otherwise, the effective Gilbert damping factor increases monotonically with the dipole field. This work demonstrates that the effective Gilbert damping factor can be analytically predicted and designed using the structure factors in magnetic metamaterials. Several possible applications of damping-controlled magnetic metamaterials are discussed.

II. DESCRIPTION OF ANALYTICAL MODEL

A. An isolated single nanoparticle

Let us suppose an isolated spherical magnetic particle. The basic formula of the LLG equation of magnetization $\boldsymbol{m} = (m_x, m_y, m_z)$ is given as

$$\frac{d\boldsymbol{m}}{dt} = -\gamma(\boldsymbol{m} \times \boldsymbol{H}) + \frac{\alpha}{m_s}\left(\boldsymbol{m} \times \frac{d\boldsymbol{m}}{dt}\right) \tag{1}$$

under the effective field $\boldsymbol{H} = (H_x, H_y, H_z)$. α is the Gilbert damping factor. γ is the gyromagnetic ratio. m_s is saturation magnetization. Equation (1) is reduced to

$$\frac{dm_x}{dt} = -\gamma(m_y H_z - m_z H_y) + \frac{\alpha}{m_s}\left(m_y\frac{dm_z}{dt} - m_z\frac{dm_y}{dt}\right), \tag{2a}$$

$$\frac{dm_y}{dt} = -\gamma(m_z H_x - m_x H_z) + \frac{\alpha}{m_s}\left(m_z\frac{dm_x}{dt} - m_x\frac{dm_z}{dt}\right), \tag{2b}$$

$$\frac{dm_z}{dt} = -\gamma(m_x H_y - m_y H_x) + \frac{\alpha}{m_s}\left(m_x \frac{dm_y}{dt} - m_y \frac{dm_x}{dt}\right). \tag{2c}$$

We assume here that the external magnetic field for resonance of an isolated magnetic particle, H_0, is applied in the z direction, and the irradiation field, which is circularly polarized electromagnetic wave, is applied in the xy plane. In the resonant state, the magnetization m_z is identical. The LLG equation is thus rewritten as

$$\frac{dm_x}{dt} = -\gamma(m_y H_0 - m_z H_y) - \frac{\alpha}{m_s} m_z \frac{dm_y}{dt}, \tag{3a}$$

$$\frac{dm_y}{dt} = -\gamma(m_z H_x - m_x H_0) + \frac{\alpha}{m_s} m_z \frac{dm_x}{dt}, \tag{3b}$$

$$\frac{dm_z}{dt} = 0. \tag{3c}$$

To differentiate Eqs. (3a) and (3b), the following expressions are obtained:

$$\frac{d^2 m_x}{dt^2} = -\gamma\left(\frac{dm_y}{dt} H_0 - m_z \frac{dH_y}{dt}\right) - \frac{\alpha}{m_s} m_z \frac{d^2 m_y}{dt^2}, \tag{4a}$$

$$\frac{d^2 m_y}{dt^2} = -\gamma\left(m_z \frac{dH_x}{dt} - \frac{dm_x}{dt} H_0\right) + \frac{\alpha}{m_s} m_z \frac{d^2 m_x}{dt^2}. \tag{4b}$$

Substituting Eqs. (3b) and (4b) into Eq. (4a), the expression of the LLG equation is reduced into the motion equation of the forced oscillation:

$$\left(1 + \frac{\alpha^2 m_z^2}{m_s^2}\right)\frac{d^2 m_x}{dt^2} + \frac{2\alpha\gamma H_0 m_z}{m_s}\frac{dm_x}{dt} + \gamma^2 H_0^2 m_x = \gamma^2 m_z H_0 H_x + \gamma m_z \frac{dH_y}{dt} + \frac{\alpha\gamma m_z^2}{m_s}\frac{dH_x}{dt}. \tag{5}$$

The right-hand side of Eq. (5) consists of functions $H_x = H_1 \cos\omega t$ and $H_y = H_1 \sin\omega t$, where H_1 and ω represents the amplitude and angular frequency of the irradiation magnetic field, respectively. By using the trigonometric synthesis formula, the right-hand side simply becomes a single term of a cosine function. As a result, Eq. (5) is rewritten as

$$\left(1 + \frac{\alpha^2 m_z^2}{m_s^2}\right)\frac{d^2 m_x}{dt^2} + \frac{2\alpha\omega_0 m_z}{m_s}\frac{dm_x}{dt} + \omega_0^2 m_x = \gamma m_z \sqrt{(\omega_0 + \omega)^2 + \frac{\alpha^2 m_z^2 \omega^2}{m_s^2}}\, H_1 \cos\omega t, \tag{6}$$

where the right-hand side is a periodic force term from the irradiated magnetic field.

The equilibrium state of the forced oscillation is given by a particular solution of Eq. (6) as

$$m_x = A\cos(\omega t + \delta), \tag{7}$$

where

$$A = \frac{\gamma m_z \sqrt{(\omega_0 + \omega)^2 + \alpha^2 m_z^2 \omega^2 / m_s^2}\, H_1}{\sqrt{\left(\omega_0^2 - \omega^2\right)^2 + 4\Gamma^2\omega^2}}, \qquad \delta = \tan^{-1}\left(\frac{2\Gamma\omega}{\omega_0^2 - \omega^2}\right), \quad \Gamma = \frac{\alpha m_z}{m_s}, \quad \omega_0 = \gamma H_0. \tag{8}$$

In the EMR, the particular solution as Eq. (7) forms the Lorentz-type absorption peak. From the peak profile $A(\omega)^2$ as a function of ω, the line width Δ of the peak is given by

$$\frac{\Delta}{\omega_0} = \sqrt{1 - 2\alpha^2 + 2\alpha\sqrt{1 - \alpha^2}} - \sqrt{1 - 2\alpha^2 - 2\alpha\sqrt{1 - \alpha^2}}, \simeq 2\alpha, \tag{9}$$

where $\sqrt{1 + 2\alpha} \simeq 1 + \alpha$ in case of $\alpha \ll 1$.

B. Magnetic metamaterials

Let us move on to magnetic metamaterials consisting of magnetic nanoparticles, as shown in Fig. 1. In the model 1 [Fig. 1(a)], the magnetic nanoparticles having identical particle volume are aligned in a simple cubic lattice. r_0 corresponds to the interparticle spacing. H_0 is applied in the z direction. The dipole interaction among nanoparticles influences not only to the dc resonance field but also to the elements of the ac irradi-

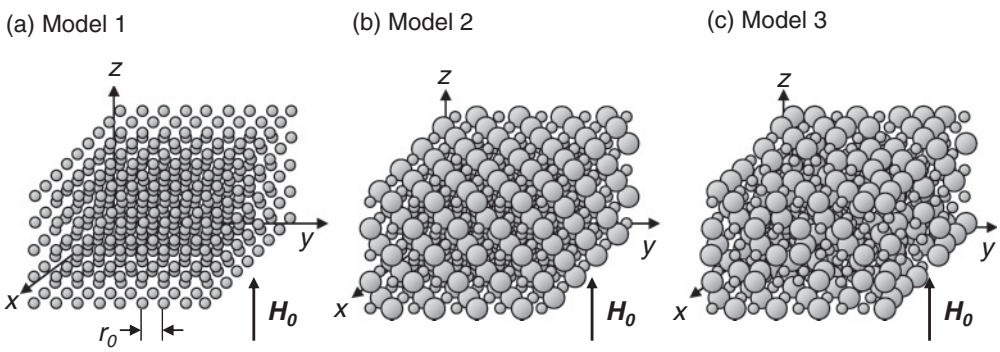

FIG. 1. Illustrations of magnetic metamaterials: (a) Model 1, (b) Model 2, and (c) Model 3. A $9 \times 9 \times 5$ simple cubic lattice with the lattice spacing r_0 is considered. Model 1 consists of single-sized particles with 8 nm in diameter, which correspond to the magnetic moment $m = 1.3 \times 10^{-16}$ emu. Contrastingly, randomness of the magnetization magnitude was introduced in Models 2 and 3. These models are composed of dual-sized particles, in which the large and small particles respectively correspond to the magnetic moment $m = 2.6 \times 10^{-16}$ emu and $m = 1.3 \times 10^{-16}$ emu. In Model 2, the large and small particles are alternately arranged just similar to an NaCl-type structure. On the other hand, in Model 3, the large and small particles randomly occupy a lattice point.

ation field. The magnetic fields in Eq. (5) are thus replaced by

$$H_x' = H_x + H_x^D, \tag{10a}$$
$$H_y' = H_y + H_y^D, \tag{10b}$$
$$H_0' = H_0 + H_z^D. \tag{10c}$$

When we suppose that the precession of the magnetization of a magnetic metamaterial is uniform as in the Kittel mode, the effective medium approximation can be applied as $\boldsymbol{m} \simeq \langle \boldsymbol{m} \rangle$ for calculations of the dipole field, $\boldsymbol{H}^D$. In this case, $\boldsymbol{H}^D$ is given by the linear combination of elements in the magnetic vector, $\langle \boldsymbol{m} \rangle$, and $\boldsymbol{H}^D$ is represented by

$$H_x^D = \langle m_x \rangle \sum_i \frac{-r_i^2 + 3x_i^2}{r_i^5} + \langle m_y \rangle \sum_i \frac{3x_i y_i}{r_i^5} + \langle m_z \rangle \sum_i \frac{3z_i x_i}{r_i^5}, \tag{11a}$$

$$H_y^D = \langle m_x \rangle \sum_i \frac{3x_i y_i}{r_i^5} + \langle m_y \rangle \sum_i \frac{-r_i^2 + 3y_i^2}{r_i^5} + \langle m_z \rangle \sum_i \frac{3y_i z_i}{r_i^5}, \tag{11b}$$

$$H_z^D = \langle m_x \rangle \sum_i \frac{3z_i x_i}{r_i^5} + \langle m_y \rangle \sum_i \frac{3y_i z_i}{r_i^5} + \langle m_z \rangle \sum_i \frac{-r_i^2 + 3z_i^2}{r_i^5}. \tag{11c}$$

The coordination of the i-th nanoparticle is represented by x_i, y_i, and z_i. The distance to the i-th nanoparticle is $r_i = \sqrt{x_i^2 + y_i^2 + z_i^2}$. Equation (5) is rewritten as

$$\left(1 + \frac{\alpha^2 \langle m_z \rangle^2}{m_s^2}\right) \frac{d^2 \langle m_x \rangle}{dt^2} + \frac{2\alpha\gamma \left(H_0 + H_z^D\right) \langle m_z \rangle}{m_s} \frac{d\langle m_x \rangle}{dt} + \gamma^2 \left(H_0 + H_z^D\right)^2 \langle m_x \rangle$$
$$= \gamma^2 \langle m_z \rangle \left(H_0 + H_z^D\right) H_x + \gamma \langle m_z \rangle \frac{dH_y}{dt} + \frac{\alpha\gamma \langle m_z \rangle^2}{m_s} \frac{dH_x}{dt} + \gamma^2 \langle m_z \rangle \left(H_0 + H_z^D\right) H_x^D + \gamma \langle m_z \rangle \frac{dH_y^D}{dt} + \frac{\alpha\gamma \langle m_z \rangle^2}{m_s} \frac{dH_x^D}{dt} \tag{12}$$

If the metamaterial is considered as a thin film, coordination z_i becomes $z_i \simeq 0$. Equation (12) is written as

$$\left(1 + \frac{\alpha^2 \langle m_z \rangle^2}{m_s^2}\right) \frac{d^2 \langle m_x \rangle}{dt^2} + \frac{2\alpha\gamma (H_0 + C_{zz} \langle m_z \rangle) \langle m_z \rangle}{m_s} \frac{d\langle m_x \rangle}{dt} + \gamma^2 (H_0 + C_{zz} \langle m_z \rangle)^2 \langle m_x \rangle$$
$$= \gamma^2 \langle m_z \rangle (H_0 + C_{zz} \langle m_z \rangle) H_x + \gamma \langle m_z \rangle \frac{dH_y}{dt} + \frac{\alpha\gamma \langle m_z \rangle^2}{m_s} \frac{dH_x}{dt} + \gamma^2 \langle m_z \rangle (H_0 + C_{zz} \langle m_z \rangle) C_{xy} \langle m_y \rangle$$
$$+ \left(\gamma C_{xy} \langle m_z \rangle + \frac{\alpha\gamma C_{xx} \langle m_z \rangle^2}{m_s}\right) \frac{d\langle m_x \rangle}{dt} + \gamma^2 \langle m_z \rangle (H_0 + C_{zz} \langle m_z \rangle) C_{xx} \langle m_x \rangle + \left(\gamma C_{yy} \langle m_z \rangle + \frac{\alpha\gamma C_{xy} \langle m_z \rangle^2}{m_s}\right) \frac{d\langle m_y \rangle}{dt}, \tag{13}$$

where

$$C_{xx} = \sum_i w_i \frac{-r_i^2 + 3x_i^2}{r_i^5}, \quad C_{xy} = \sum_i w_i \frac{3x_i y_i}{r_i^5},$$
$$C_{yy} = \sum_i w_i \frac{-r_i^2 + 3y_i^2}{r_i^5}, \quad C_{zz} = \sum_i w_i \frac{-1}{r_i^3}. \tag{14}$$

w_i corresponds to the weight parameter defined by the volume of the nanoparticles, enabling us to treat dual- or multisize particle systems as shown in Figs. 1(b) and 1(c). Coefficients described by Eq. (14) are structure factors of magnetic metamaterials.

For Eq. (13), in the case of equilibrium state of precession, elements $\langle m_x \rangle$ and $\langle m_y \rangle$ satisfy the following relations:

$$\langle m_y \rangle = -\frac{1}{\omega} \frac{d\langle m_x \rangle}{dt}, \quad \frac{d\langle m_y \rangle}{dt} = \omega \langle m_x \rangle. \tag{15}$$

Taking these relations into account, Eq. (13) is expressed for a single variable $\langle m \rangle \equiv \langle m_x \rangle$ and written as

$$(1 + \alpha^2) \frac{d^2 \langle m \rangle}{dt^2} + 2\alpha\omega_D \frac{d\langle m \rangle}{dt} + \omega_D^2 \langle m \rangle$$
$$= \gamma m_s \left(\omega_D H_x + \frac{dH_y}{dt} + \alpha \frac{dH_x}{dt}\right)$$
$$+ \gamma m_s \left(C_{xy} + \alpha C_{xx} - \frac{\omega_D C_{xy}}{\omega}\right) \frac{d\langle m \rangle}{dt}$$
$$+ \gamma m_s (\omega C_{yy} + \alpha\omega C_{xy} + \omega_D C_{xx}) \langle m \rangle, \tag{16}$$

where the approximation for $\langle m_z \rangle \simeq m_s$ is used. We changed the expression to the time domain using a variable transformation of $\gamma(H_0 + C_{zz} m_s) = \omega_D$, Kittel's equation.

Equation (16) is analogous to Eq. (5), which is the equation of forced oscillation. However, the second and third terms in the right-hand side of Eq. (16) have no counterpart in Eq. (5). We should note here that the effective medium approximation

is quite useful. The second and third terms in the right-hand side of Eq. (16) become the equivalent rank of the derivation for the second and third terms in the left-hand side and can be moved to the left-hand side. Finally, Eq. (16) becomes

$$(1+\alpha^2)\frac{d^2\langle m\rangle}{dt^2} + 2\alpha'\omega_D'\frac{d\langle m\rangle}{dt} + {\omega_D'}^2\langle m\rangle = f\cos\omega t, \tag{17}$$

where

$$\omega_D' = \sqrt{\omega_D^2 - \gamma m_s(\omega C_{yy} + \alpha\omega C_{xy} + \omega_D C_{xx})}, \tag{18}$$

$$2\alpha'\omega_D' = 2\alpha\omega_D - \gamma m_s\left(C_{xy} + \alpha C_{xx} - \frac{\omega_D C_{xy}}{\omega}\right). \tag{19}$$

For magnetic metamaterials, we expect the magnetic permeability to be controlled. The magnitude of magnetic permeability is determined by $A(\omega)^2$. Namely, the control of α' brings about the control of the magnetic permeability $\mu = 1 + \chi$, where χ is the magnetic susceptibility. An analogy between Eqs. (6) and (17) allows us to express the line width of the EMR signal in the magnetic metamaterials as

$$\frac{\Delta'}{\omega_D'} \simeq 2\alpha'. \tag{20}$$

Equations (18)–(20) reveal that the line width can be described using the structure factors given as Eq. (14). Effective Gilbert damping can thus be designed analytically by internal structures of the metamaterials.

III. NUMERICAL SIMULATION

Equation (17) shows that the state of the magnetic precession is strongly affected by the summation of the dipole field in structure factors as described by Eq. (14). The dipole field is dominated by the distance between particles and by the magnitude of the magnetic moment in the particle. Previously we studied the effect of the distance between particles.[15] In this calculation, we focus our attention on the influence of the magnitude of the moment. In order to visualize the behavior of the analytical model, we carried out the numerical calculation for a magnetic metamaterial consisting of magnetic nanoparticles, as shown in Figs. 1(a)–1(c).

The nanoparticles are arranged in a $N_x \times N_y \times N_z$ simple cubic lattice with the lattice spacing r_0. The magnetic dipole interaction among nanoparticles depends on the distance r_0 and the number of particles involved in the summation $\sum_{|\pm i|<N_x}$ [see Eq. (11a)]. In the case of $r_0 = 10$ nm, $\sum_{|\pm i|<N_x=9}$ is very similar to $\sum_{|\pm i|<N_x=10}$ in terms of the dipole field. Therefore, to save the resource in the numerical calculation, we chose the size of the nanoparticle array to be $N_x = N_y = 9$. We assume $N_z = 5$ in the present calculation.

Model 1 as shown in Fig. 1(a) consists of single-sized particles with 8 nm in diameter, which correspond to the magnetic moment $m = 1.3 \times 10^{-16}$ emu. Contrastingly, randomness of the magnetization magnitude was introduced in model 2 [Fig. 1(b)] and model 3 [Fig. 1(c)]. These models are composed of dual-sized particles, in which the large and small particles, respectively, correspond to the magnetic moment $m = 2.6 \times 10^{-16}$ emu and $m = 1.3 \times 10^{-16}$ emu. In model 2, the large and small particles are alternately arranged just similar to an NaCl-type structure. On the other hand, in model 3, the large and small particles randomly occupy a lattice point.

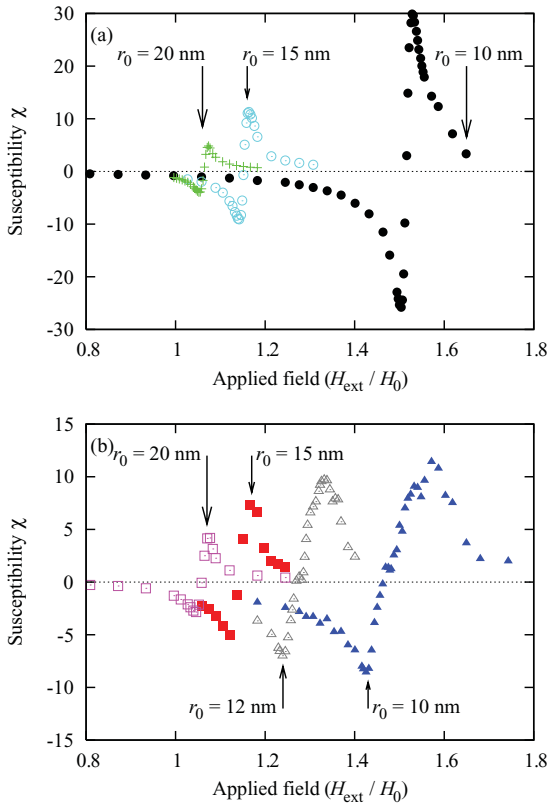

FIG. 2. (Color online) Line profile of the susceptibility χ in field sweep with (a) Model 2 and (b) Model 3. Lattice constant r_0 is set to be $r_0 = 10$ nm (filled circles and filled triangles), 12 nm (open triangles), 15 nm (open circles and filled squares) and 20 nm (crosses and open squares).

In the numerical calculation, the mirror boundary condition is applied in x and y directions, and the open boundary condition is applied in the z direction. These settings reproduce magnetic metamaterials in the form of a thin film including the magnetic nanoparticles. The LLG equation of each particle is directly solved using the forward difference method and taking account of the dipole interaction among the magnetic particles. γ and α are assumed to be 1.76×10^7 $\mathrm{Oe}^{-1}\mathrm{s}^{-1}$ and 0.010, respectively.

Figure 2 shows the peak profiles of magnetic susceptibility in a field sweep. The applied field is normalized by H_0, where H_0 represents the resonant field of the isolated nanoparticle at the frequency $\omega_0/2\pi = 9$ GHz. In the case of model 2 [Fig. 2(a)], r_0 is varied in the range of $r_0 = 10$ nm (filled circles), 15 nm (open circles), and 20 nm (crosses). As r_0 decreases, the maximum value of χ increases. This is brought about by an increase in the magnetic moment per unit volume. The apparent resonant field H_0', where H_0' is defined as the zero cross point of χ, increases with a decrease in r_0. The increase in H_0' is traced back to an increase in the magnetic dipole field among nanoparticles.[15] We see that the curves of the peak profiles in Fig. 2(a) are smooth.

Contrastingly, in the case of model 3 with $r_0 = 10$ nm (filled triangles), 12 nm (open triangles), 15 nm (filled squares), and 20 nm (open squares) [Fig. 2(b)], the peak profiles are not smooth curves. The value of χ depends on the randomization procedure in this calculation. Each data point is thus given by the average of three trials except near the resonance field. Near the resonant state, the number of trials increases to ten. The maximum χ is smaller than that in model 2. For the resonance field that is given by the crossing point at $\chi = 0$, particles with $r_0 = 15$ and 20 nm indicate a similar value in comparison with models 2 and 3. However, in the case of $r_0 = 10$ nm, the resonance field of model 3 is slightly smaller than that of model 2. On the other hand, the maximum (or minimum) χ of model 3 is drastically smaller than that of model 2 when r_0 decreases to 10 nm.

IV. DISCUSSION

The calculated line profiles of models 2 and 3 at $r_0 = 10$ nm are simultaneously plotted in Fig. 3. Calculated data points are fitted by the function of A^2, where the amplitude A is defined in the particular solution as the form of Eq. (7). The fitting to Eq. (20) brings about an effective Gilbert damping factor α'. As a control, we carried out numerical calculation of model 1 with single-sized particles, although the line profile is not shown in this paper. Obtained values of α', as well as the resonant field (H_0'/H_0), are listed in Table I.

When the isolated particles are assembled into model 1, α' increases from 0.010 to 0.020. This increase is caused by the magnetic dipole field among particles, i.e., demagnetization field in a film, corresponding to the simple dipole broadening.[17] Indeed, as shown in Table I, H_0'/H_0 increases in model 1. The models with the dual-sized particle system (models 2 and 3) show an additional increase in H_0'/H_0. Obviously, the total magnetic moment in the dual-sized particles system becomes larger than that in the single-sized particles system, leading to an increase in the strength of the dipole field; this brings about the additional increase in H_0'/H_0. Table I shows that H_0'/H_0 is mostly similar between models 2 and 3; the dipole field is almost the same in these models. However, Table I demonstrates how an increase in the dipole field affects α'

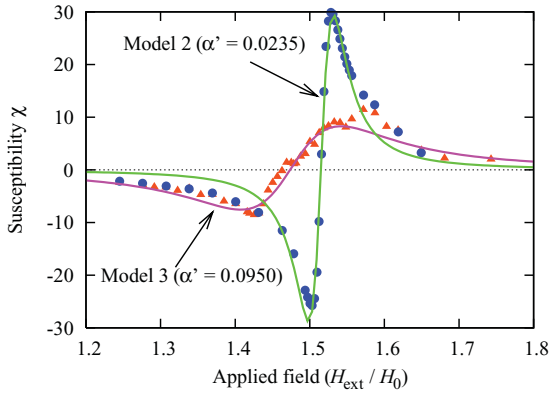

FIG. 3. (Color online) Comparison between Model 2 (green line and blue circles) and Model 3 (pink line and red triangles) when $r_0 = 10$. Effective Gilbert damping factor α' is obtained from the fitting curves.

TABLE I. Model, particle size, distribution, the effective Gilbert damping factor α', and the resonant field H_0'/H_0.

Model	Particle size	Distribution	α'	H_0'/H_0
isolated particle	–	–	0.010	1.000
Model 1	single	–	0.020	1.218
Model 2	dual	periodic	0.024	1.515
Model 3	dual	random	0.095	1.480

differently in models 2 and 3. As a result, the α' of model 2 is much smaller than that of model 3, even though H_0'/H_0 of model 2 is almost the same as that of model 3.

Analytically, this discrepancy between models 2 and 3 can be understood using Eqs. (17)–(19). The static dipole field influences the ω_D through C_{zz}, which is the major factor of the peak shift in H_0'/H_0 expressed by the Kittel equation. In the static Kittel equation, a shift in H_0'/H_0 due to the dipole field does not bring about a change in line width, i.e., in α'. Contrastingly, a dynamic approximation based on the LLG equation shown as Eq. (17) indicates that an increase in the dynamic dipole field, i.e., H_0'/H_0, accompanies an apparent broadening of line width because of the second term (damping term) of the left-hand side. The dynamic dipole field is characterized by C_{xx}, C_{yy}, and C_{xy}. These structure factors give rise to the peak shift in the $H_0' = \omega_D'/\gamma$. As shown in Eq. (18), an increase in C_{xx}, C_{yy}, and C_{xy} brings about a decrease in ω_D'. On the other hand, how these structure factors affect the α' is described in Eq. (19); we notice here that an increase in C_{xx} and C_{yy} causes a decrease in α' but that in C_{xy} results in an increase in α'. α' is influenced intricately by C_{xx}, C_{yy}, and C_{xy}. In other words, α' can be analytically predicted and designed using the structure factors.

In the magnetic metamaterials, the structure factor is spatially strengthened or weakened like an interference. It is worth mentioning here that the spacial variation of magnetic moments give rise to the variation in α', which is very similar to the variable α of magnetic metals owing to the spatial variation of spins.[18,19] As well as the dipole field among nanoparticles, ac current and spin current could be the interacting field leading to the manipulation of the damping factor through electric current. This work introduces a new relationship between metamaterials and spintronics. Another important point in the dynamic approximation is the cooperation of a dipole field with the magnetization precession; the synchronization of the vibrating dipole field to the magnetization precession is the origin of the variation in α'. This synchronization allow us to justify effective medium approximation and, therefore, to derive analytically α' of magnetic metamaterials. Otherwise, numerical calculation should be used to extract α'.

V. CONCLUSIONS

We have studied theoretically the LLG equation in magnetic metamaterials and numerically the dynamics of the magnetization. Our results revealed that one can control Gilbert damping and magnetic permeability through the design of the internal structures of magnetic metamaterials. The origin of the variation in the effective Gilbert damping factor is the interacting field synchronized to the magnetization precession.

The increase in interacting dipole field basically leads to an increase in the effective Gilbert damping factor. Nevertheless, it is found that a metamaterial consisting of dual-sized particles has almost the same effective Gilbert damping factor with that of single-sized particles although an increase in the interacting dipole field. This work demonstrates that the effective Gilbert damping factor can be analytically designed using the structure factors in magnetic metamaterials, opening an avenue to a new relationship between metamaterials and spintronics.

ACKNOWLEDGMENT

The authors acknowledge the financial support by KAKENHI (Grant No. 23654124) from the MEXT, Japan.

*mitsumata@solid.apph.tohoku.ac.jp
†tomita@ms.naist.jp

[1] D. R. Smith, J. B. Pendry, and M. C. K. Wiltshire, Science **305**, 788 (2004).
[2] J. B. Pendry, A. J. Holden, D. R. Robbins, and M. J. Stewart, IEEE Trans. Microwave Theory Tech. **47**, 2075 (1999).
[3] D. R. Smith, W. J. Padilla, D. C. Vier, S. C. Nemat-Nasser, and S. Schultz, Phys. Rev. Lett. **84**, 4184 (2000).
[4] S. T. Chui and L. Hu, Phys. Rev. B **65**, 144407 (2002).
[5] T. L. Gilbert, Phys. Rev. **100**, 1243 (1955); L. D. Landau, E. M. Lifshitz, and L. P. Pitaevski, *Statistical Physics*, Part 2, 3rd ed. (Pergamon, Oxford, 1980).
[6] S. Mizukami, Y. Ando, and T. Miyazaki, Phys. Rev. B **66**, 104413 (2002).
[7] Y. Tserkovnyak, A. Brataas, and G. E. W. Bauer, Phys. Rev. Lett. **88**, 117601 (2002).
[8] H. Kohno, G. Tatara, and J. Shibata, J. Phys. Soc. Jpn. **75**, 113706 (2006).
[9] M.-C. Ciornei, J. M. Rubi, and J.-E. Wegrowe, Phys. Rev. B **83**, 020410(R) (2011).
[10] I. Mayergoyz, G. Bertotti, and C. Serpico, Phys. Rev. B **83**, 020402(R) (2011).
[11] K. Akamatsu, H. Shinkai, S. Ikeda, H. Nawafune, and S. Tomita, J. Am. Chem. Soc. **127**, 7980 (2005).
[12] S. Tomita, K. Akamatsu, H. Shinkai, S. Ikeda, H. Nawafune, C. Mitsumata, T. Kashiwagi, and M. Hagiwara, Phys. Rev. B **71**, 180414(R) (2005).
[13] S. Tomita, P. E. Jönsson, K. Akamatsu, H. Nawafune, and H. Takayama, Phys. Rev. B **76**, 174432 (2007).
[14] C. Mitsumata and S. Tomita, Appl. Phys. Lett. **91**, 223104 (2007).
[15] C. Mitsumata, S. Tomita, M. Hagiwara, and K. Akamatsu, J. Phys. Condens. Mater **22**, 013001 (2010).
[16] C. Kittel, *Introduction to Solid State Physics*, 7th ed. (Wiley, New York, 1995).
[17] J. H. Van Vleck, Phys. Rev. **74**, 1168 (1948).
[18] A. Takeuchi, K. Hosono, and G. Tatara, Phys. Rev. B **81**, 144405 (2010).
[19] D. Miura and A. Sakuma, J. Appl. Phys. **109**, 07C909 (2011).